Supporting Information for:

RAFT Dispersion Polymerization of Methyl Methacrylate in Mineral Oil: High Glass Transition Temperature of the Core-forming Block Constrains the Evolution of Copolymer Morphology

Csilla György, Chloe Verity, Thomas J. Neal, Matthew J. Rymaruk, Erik J. Cornel, Timothy Smith, David J. Growney and Steven P. Armes*

Table of Contents

Experimental Section

Materials

Methyl methacrylate (MMA, 99%) was purchased from Alfa Aesar (Germany), passed through basic alumina to remove its inhibitor and then stored at –20 °C prior to use. Lauryl methacrylate (LMA), dicumyl peroxide (DCP), $CDCl_3$ and *n*-dodecane were purchased from Merck (UK) and used as received. Stearyl methacrylate (SMA) was purchased from Santa Cruz Biotechnology, Inc. (USA). 2,2'-Azoisobutyronitrile (AIBN) was obtained from Molekula (UK) and *tert*-butyl peroxy-2-ethylhexanoate (T21s) was purchased from AkzoNobel (The Netherlands). CD_2Cl_2 was purchased from Goss Scientific (UK). Tetrahydrofuran was obtained from VWR Chemicals (UK). Methanol and toluene were purchased from Fisher Scientific (UK). 4-Cyano-4(dodecylthiocarbonothioylthio)pentanoate (MCDP) and Group III hydroisomerized mineral oil (viscosity = 4.3 cSt at 100 °C) were kindly provided by The Lubrizol Corporation Ltd. (Hazelwood, Derbyshire, UK).

Synthesis of poly(lauryl methacrylate) (PLMA) precursor block *via* RAFT solution polymerization in toluene

$PLMA_{22}$, $PLMA_{30}$ and $PLMA_{41}$ precursor blocks were prepared at 50% w/w solids (see **Table S1**). A typical synthesis of $PLMA_{22}$ was conducted as follows. LMA (48.7 g; 191.5 mmol), MCDP (4.0 g; 9.6 mmol; target DP = 20), AIBN (315 mg; 1.9 mmol; MCDP/AIBN molar ratio = 5.0) and toluene (53.0 g) were weighed into a 250 mL round-bottomed flask. The sealed flask was purged with nitrogen for 30 min and immersed in a preheated oil bath at 80 ºC. The reaction solution was stirred continuously and the ensuing polymerization was quenched after 4.5 h by exposing the reaction solution to air and cooling the flask to room temperature. A final LMA conversion of 91% was determined by ^{1}H NMR spectroscopy. In order to remove residual monomer, the crude polymer was purified by three consecutive precipitations into a ten-fold excess of methanol (with redissolution in THF after precipitation). The mean DP of the precursor block was calculated to be 22 by using ^{1}H NMR spectroscopy to compare the three methyl protons assigned to the trithiocarbonate end-group at 3.7 ppm to the two

oxymethylene protons attributed to PLMA at 3.80–4.20 ppm (see **Figure S1**). Kinetic studies for this polymerization were also performed (see **Figure S2**). THF GPC analysis using a refractive index detector and a series of near-monodisperse poly(methyl methacrylate) standards indicated an M_n of 6 000 g mol^{-1} and an M_w/M_n of 1.13. $PSMA_{10}$ and $PSMA_{37}$ precursor blocks were synthesized by following the previously reported synthesis protocol.[1,2]

Two-pot synthesis of poly(lauryl methacrylate)-poly(methyl methacrylate) ($PLMA_{22}$-$PMMA_{69}$) diblock copolymer nanoparticles *via* RAFT dispersion polymerization of MMA in mineral oil

The following example of a two-pot synthesis targeting $PLMA_{22}$-$PMMA_{69}$ nanoparticles at 20% w/w solids is representative and was conducted as follows. $PLMA_{22}$ precursor (0.20 g; 33.25 μmol), T21s initiator (2.40 mg; 11.08 μmol; 10.0% v/v in mineral oil) and mineral oil (1.74 g) were weighed into a glass vial and purged with nitrogen for 30 min. MMA monomer (0.25 mL; 2.33 mmol) was degassed separately then added to the reaction mixture *via* syringe. The sealed vial was immersed in a preheated oil bath at 90 °C and the reaction mixture was magnetically stirred for 17 h. ^{1}H NMR analysis indicated 98% MMA conversion by comparing the integrated methyl signal of the monomer at 3.75–3.78 ppm to the integrated methyl signal of the polymer at 3.50–3.72 ppm. THF GPC analysis indicated an M_n of 14 800 g mol^{-1} and an M_w/M_n of 1.14. To construct a pseudo-phase diagram for $PLMA_y$-$PMMA_x$ nano-objects prepared in mineral oil, a range of diblock copolymer compositions were targeted using $PLMA_{22}$, $PLMA_{30}$ and $PLMA_{41}$ precursors in turn at 20% w/w solids. In each case, the same mass of $PLMA_y$ precursor was used and the MMA/$PLMA_y$ molar ratio and volume of mineral oil were adjusted accordingly. The effect of varying the synthesis temperature on the copolymer morphology was studied by using the same protocol to target diblock copolymer compositions at either 70 °C (with AIBN initiator) or 115 °C (with DCP initiator). For syntheses performed at 115 °C, the round-bottomed flask was sealed with a plastic cap rather than a rubber septum in order to prevent evaporative loss of MMA monomer (boiling point = 101 °C). Furthermore, a series of $PSMA_y$-$PMMA_x$ nanoparticles were prepared at 20% w/w solids in mineral oil using either a $PSMA_{10}$ or a $PSMA_{37}$ precursor at 90 °C using the same protocol.

One-pot synthesis of poly(lauryl methacrylate)-poly(methyl methacrylate) ($PLMA_{19}$-$PMMA_{69}$) nanoparticles

A typical one-pot PISA synthesis of $PLMA_{19}$-$PMMA_{69}$ nanoparticles at 20% w/w solids in mineral oil was conducted as follows. LMA (2.44 g; 9.58 mmol; target 60% w/w solids), MCDP (0.20 g; 478.8 μmol; target degree of polymerization = 20) and T21s initiator (20.7 mg; 95.8 μmol; dissolved at 10% v/v in mineral oil) were dissolved in mineral oil (1.79 g). The reaction mixture was sealed in a 100 mL round-bottomed flask and deoxygenated with nitrogen gas for 30 min. The flask was then placed in a pre-heated oil bath at 90 °C for 6 h (final LMA conversion = 97%; M_n = 6 300 g mol^{-1}; M_w/M_n = 1.11) (see **Figure S3**). T21s initiator (34.5 mg; 159.6 μmol; dissolved at 10% v/v in mineral oil) was dissolved in mineral oil (22.45 g) and purged with nitrogen gas for 30 min before being added to the reaction solution at 97%

LMA conversion. MMA monomer (3.57 mL; 33.52 mmol; target degree of polymerization = 70) was degassed separately and then added to the reaction solution *via* syringe. The reaction mixture was heated at 90 °C for a further 17 h. ^{1}H NMR studies confirmed a final MMA conversion of 99% (see **Figure S3)** while GPC studies indicated an M_n of 14 500 g mol^{-1} and an M_w/M_n of 1.11. A series of PLMA$_{19}$-PMMA$_x$ nanoparticles were also prepared at 30% w/w solids in mineral oil and at 20% w/w solids in *n*-dodecane using essentially the same synthesis protocol.

NMR Spectroscopy

^{1}H NMR spectra were recorded in either CD_2Cl_2 or $CDCl_3$ using a 400 MHz Bruker Avance spectrometer. Typically, 64 scans were averaged per spectrum. For the kinetic study of the synthesis of PLMA$_{19}$-PMMA$_{100}$ nano-objects at 20% w/w solids in mineral oil, aliquots were extracted from the reaction mixture every 10 min for the first 90 min then at 30 min intervals for a further 60 min. Each aliquot was diluted with CD_2Cl_2 prior to ^{1}H NMR analysis.

Gel Permeation Chromatography (GPC)

Molecular weight distributions (MWDs) were assessed by GPC using THF as an eluent. The GPC system was equipped with two 5 μm (30 cm) Mixed C columns and a WellChrom K-2301 refractive index detector operating at 950 ± 30 nm. The THF mobile phase contained 2.0% v/v triethylamine and 0.05% w/v butylhydroxytoluene (BHT) and the flow rate was fixed at 1.0 ml min^{-1}. A series of twelve near-monodisperse poly(methyl methacrylate) standards (M_p values ranging from 800 to 2 200 000 g mol^{-1}) were used for column calibration in combination with a refractive index detector.

Dynamic Light Scattering (DLS)

DLS studies were performed using a Zetasizer Nano ZS instrument (Malvern Instruments, UK) at a fixed scattering angle of 173°. Copolymer dispersions were diluted in *n*-dodecane (0.10% w/w) prior to light scattering studies at 20 °C. The intensity-average diameter and polydispersity of the nanoparticles were calculated by cumulants analysis of the experimental correlation function using Dispersion Technology Software version 6.20. Data were averaged over ten runs each of thirty seconds duration. It is emphasized that DLS assumes a spherical morphology. Thus, the DLS diameter determined for anisotropic nanoparticles such as worms is a 'sphere-equivalent' value that does not indicate the worm length or the worm width. Nevertheless, DLS can be used to monitor a thermally-induced worm-to-sphere transition by monitoring the reduction in the apparent diameter as a function of temperature.[3]

Transmission Electron Microscopy (TEM)

TEM studies were conducted using a Philips CM 100 instrument operating at 100 kV and equipped with a Gatan 1k CCD camera. A single droplet of a 0.10% w/w copolymer dispersion was placed onto a carbon-coated copper grid and allowed to dry, prior to exposure to ruthenium(VIII) oxide vapor for 7 min at 20 °C.[4] This heavy metal compound acts as a positive stain for the core-forming PMMA block to improve

contrast. The ruthenium(VIII) oxide was prepared as follows: ruthenium(IV) oxide (0.30 g) was added to water (50 g) to form a black slurry; addition of sodium periodate (2.0 g) with continuous stirring produced a yellow solution of ruthenium(VIII) oxide within 1 min at 20 °C.

Small-angle X-ray scattering (SAXS)

SAXS patterns were recorded using a Xeuss 2.0 laboratory beamline (Xenocs, Grenoble, France) equipped with a MetalJet X-ray source (GaK_α radiation, wavelength λ = 1.34 Å, with q ranging from 0.004 to 0.300 Å^{-1}, where $q = 4\pi.\sin\theta/\lambda$ is the length of the scattering vector and θ is one-half of the scattering angle) and a 2D Pilatus 1M pixel detector (Dectris, Baden-Daettwil, Switzerland). A glass capillary of 2.0 mm diameter was used as a sample holder. Scattering data were reduced using software supplied by the SAXS instrument manufacturer and were further analyzed using Irena SAS macros for Igor Pro.[5]

Differential scanning calorimetry (DSC)

Measurements were performed using a TA DSC25 Discovery series instrument operating from 0 to 180 °C at a rate of 5 °C min^{-1} using aluminum T_{zero} pans and T_{zero} hermetic lids for both PMMA homopolymers and PLMA$_{22}$-PMMA$_x$ diblock copolymers. Instrument calibration was performed using an indium standard. Purified PLMA$_{22}$-PMMA$_x$ (where x is 69, 97, 139 or 194) powders were obtained after three consecutive precipitations of the as-synthesized diblock copolymer dispersion into a ten-fold excess of methanol (with redissolution in THF after each precipitation), followed by isolation *via* filtration and drying under vacuum for 24 h. For DSC analysis, each diblock copolymer (or PMMA homopolymer) was subjected to two heating/cooling cycles: the first cycle ensured removal of residual organic solvent, and the glass transition temperature was determined during the second cycle.

Oscillatory Rheology

An Anton Paar MCR 502 rheometer (equipped with TruGap functionality for online monitoring of the geometry gap), a variable-temperature Peltier plate, Peltier hood and a 50 mm 2° stainless cone was used for the rheology experiments. The storage (G') and loss (G'') moduli were determined as a function of temperature at a heating rate of 2 °C min^{-1}, a fixed strain amplitude of 1.0%, and an angular frequency of 10 rad s^{-1}. The sample gap was 207 μm.

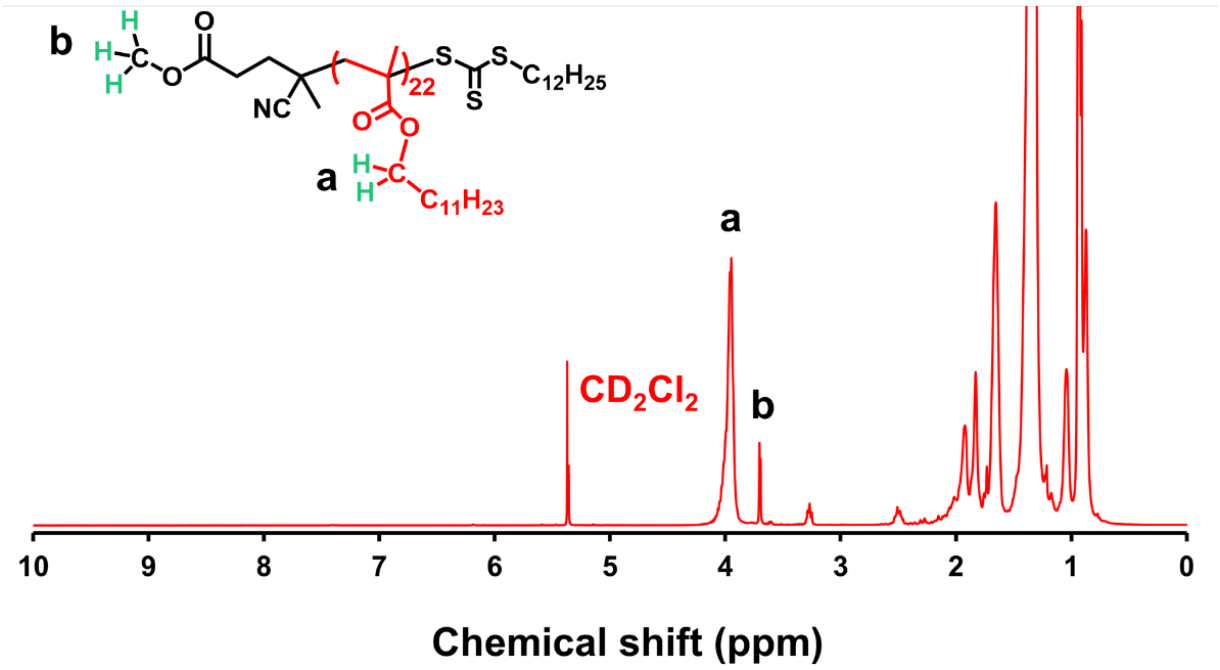

Figure S1. Assigned ^{1}H NMR spectrum recorded in CD_2Cl_2 for the $PLMA_{22}$ precursor prepared *via* RAFT solution polymerization in toluene using the MCDP RAFT agent.

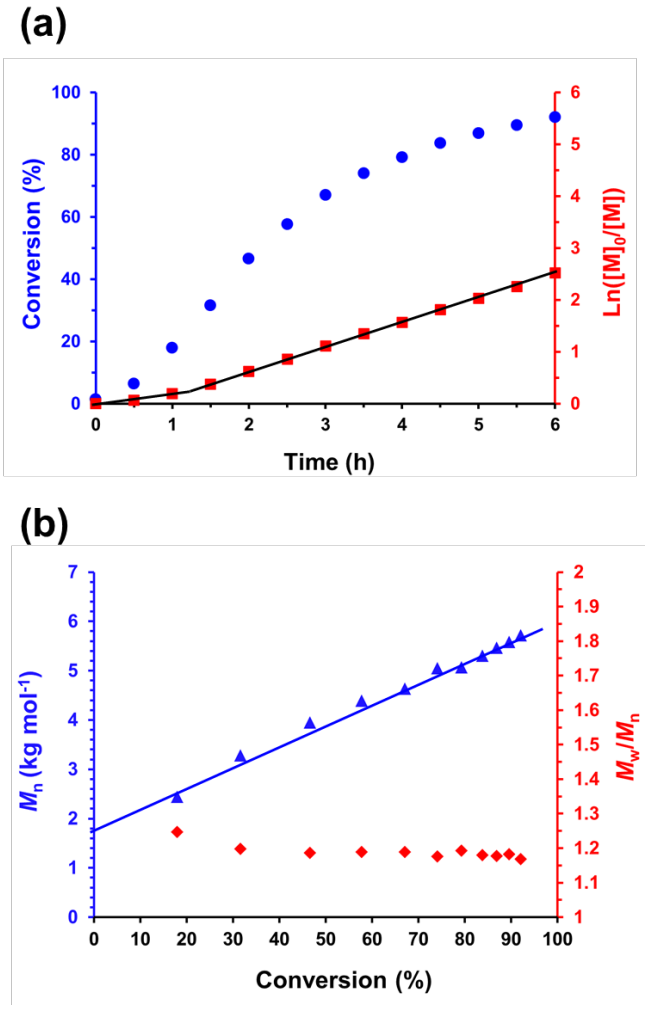

Figure S2. RAFT solution polymerization of LMA in toluene at 50% w/w solids and 80 °C using MCDP as a RAFT agent (target PLMA DP = 20; MCDP/initiator molar ratio = 5.0). **(a)** Conversion *vs*. time (blue circles) and corresponding ln([M]$_0$/[M]) *vs*. time (red squares) plots. **(b)** Evolution in M_n (blue triangles) and M_w/M_n (red diamonds) obtained by THF GPC analysis using a series of near-monodisperse poly(methyl methacrylate) calibration standards.

Table S1. Summary of the reaction times, conversions and GPC data obtained for three PLMA$_x$ precursors prepared at 50% w/w solids in toluene at 80 °C.

Target DP of PLMA precursor	Reaction time (h)	LMA Conversion (%)	THF GPC		Final DP of PLMA precursor
			M_n (g mol^{-1})	M_w/M_n	
20	4.5	91	6,000	1.13	22
40	4.5	90	8,400	1.13	30
50	5.5	89	11,300	1.12	41

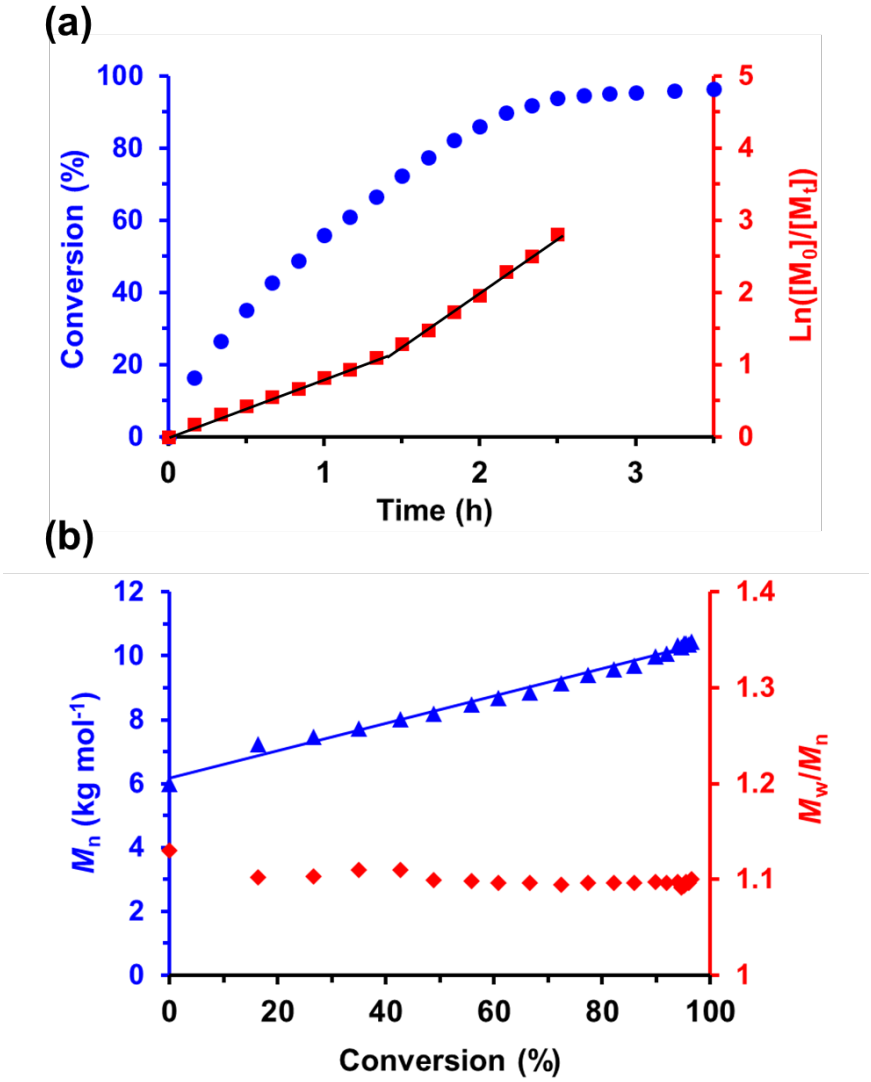

Figure S3. (a) Conversion *vs*. time curve (blue circles) and the corresponding ln([M_0]/[M_t]) *vs*. time plot (red squares) for the RAFT dispersion polymerization of MMA at 90 °C targeting $PLMA_{22}$-$PMMA_{30}$ spheres using a $PLMA_{22}$ precursor at 20% w/w solids in mineral oil using the two-pot protocol. **(b)** Evolution of M_n (blue triangles) and M_w/M_n (red diamonds) with monomer conversion for this PISA formulation. Micellar nucleation was determined at 80 min; MMA conversion = 67%; PMM DP ~ 20.

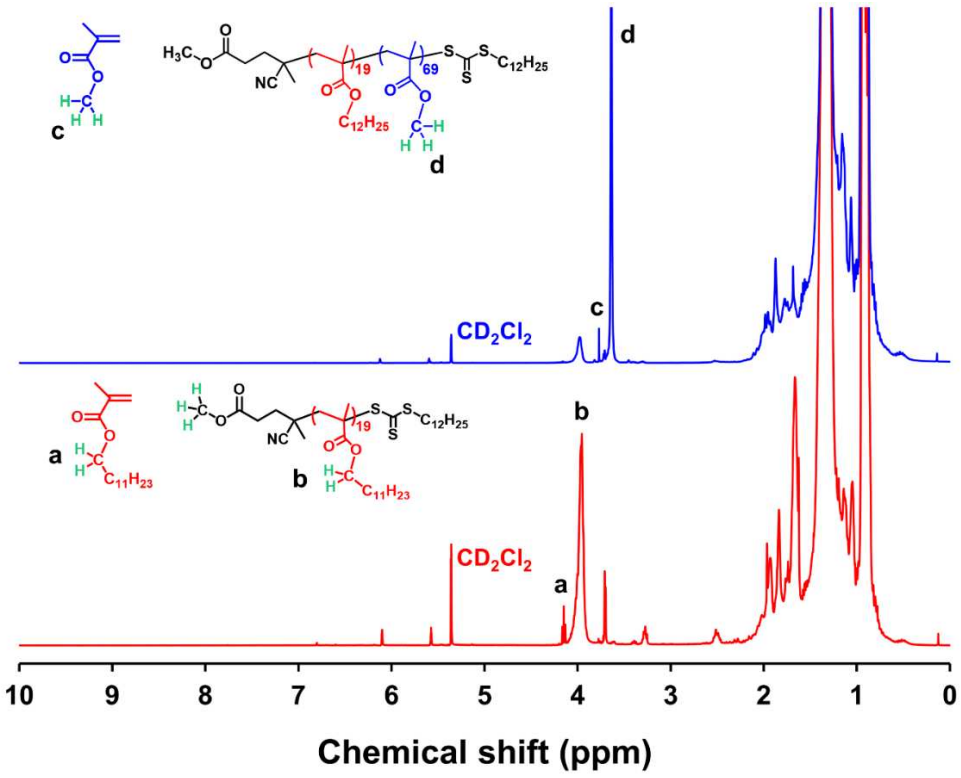

Figure S4. Assigned ^{1}H NMR spectra recorded in CD_2Cl_2 for the $PLMA_{19}$ precursor (red spectrum; LMA conversion = 97%) and the $PLMA_{19}$-$PMMA_{69}$ diblock copolymer (blue spectrum; MMA conversion = 99%) prepared using the one-pot synthesis protocol at 20% w/w solids in mineral oil at 90 °C.

Table S2. Summary of the GPC, DLS and TEM data obtained for a series of $PLMA_{19}$-$PMMA_x$ nano-objects prepared using the one-pot protocol at 20% w/w solids in mineral oil at 90 °C.

Target Composition	LMA Conversion (%)	THF GPC		MMA Conversion (%)	THF GPC		Final Composition	DLS		TEM Morphology
		M_n (g mol^{-1})	M_w/M_n		M_n (g mol^{-1})	M_w/M_n		D_h (nm)	PDI	
$PLMA_{20}$-$PMMA_{20}$	97	6,000	1.11	98	8,100	1.11	$PLMA_{19}$-$PMMA_{20}$	15	0.37	Chains and Spheres
$PLMA_{20}$-$PMMA_{50}$	97	5,900	1.11	98	10,800	1.11	$PLMA_{19}$-$PMMA_{49}$	21	0.09	Spheres
$PLMA_{20}$-$PMMA_{70}$	97	6,300	1.11	99	14,500	1.11	$PLMA_{19}$-$PMMA_{69}$	41	0.11	Spheres and Short Worms
$PLMA_{20}$-$PMMA_{90}$	97	6,000	1.11	99	16,200	1.12	$PLMA_{19}$-$PMMA_{89}$	272	0.65	Spheres and Short Worms
$PLMA_{20}$-$PMMA_{100}$	97	6,300	1.11	99	17,600	1.11	$PLMA_{19}$-$PMMA_{99}$	123	0.22	Spheres and Short Worms
$PLMA_{20}$-$PMMA_{120}$	97	5,900	1.11	99	18,300	1.14	$PLMA_{19}$-$PMMA_{119}$	549	0.66	Aggregated Spheres
$PLMA_{20}$-$PMMA_{140}$	97	6,000	1.11	99	22,600	1.17	$PLMA_{19}$-$PMMA_{139}$	658	0.61	Aggregated Spheres
$PLMA_{20}$-$PMMA_{200}$	97	6,200	1.11	99	27,500	1.21	$PLMA_{19}$-$PMMA_{198}$	586	0.54	Aggregated Spheres

Table S3. Summary of the GPC, DLS and TEM data obtained for two series of $PLMA_{22}$-$PMMA_x$ and $PLMA_{30}$-$PMMA_x$ nano-objects prepared at 20% w/w solids in mineral oil at 90 °C using the two-pot protocol.

Target Composition	Synthesis Temperature (°C)	MMA Conversion (%)	THF GPC		DLS		TEM Morphology
			M_n (g mol^{-1})	M_w/M_n	D_h (nm)	PDI	
$PLMA_{22}$-$PMMA_{20}$	90	97	9,200	1.11	18	0.15	Spheres
$PLMA_{22}$-$PMMA_{30}$	90	97	10,600	1.12	21	0.05	Spheres
$PLMA_{22}$-$PMMA_{40}$	90	97	11,600	1.12	30	0.19	Spheres
$PLMA_{22}$-$PMMA_{50}$	90	99	12,400	1.13	37	0.10	Spheres and Short Worms
$PLMA_{22}$-$PMMA_{60}$	90	98	13,000	1.12	54	0.14	Spheres and Short Worms
$PLMA_{22}$-$PMMA_{70}$	90	98	14,800	1.14	260	0.73	Short Worms
$PLMA_{22}$-$PMMA_{80}$	90	98	16,200	1.16	782	0.93	Short Worms
$PLMA_{22}$-$PMMA_{90}$	90	98	16,900	1.17	452	0.64	Short Worms
$PLMA_{22}$-$PMMA_{100}$	90	97	17,100	1.16	973	0.65	Short Worms
$PLMA_{22}$-$PMMA_{110}$	90	98	18,700	1.17	1236	0.84	Aggregated Spheres
$PLMA_{22}$-$PMMA_{140}$	90	99	22,100	1.25	1991	1.00	Aggregated Spheres
$PLMA_{22}$-$PMMA_{200}$	90	97	27,800	1.36	6094	0.68	Aggregated Spheres
$PLMA_{30}$-$PMMA_{30}$	90	98	15,700	1.11	24	0.06	Spheres
$PLMA_{30}$-$PMMA_{50}$	90	98	17,200	1.12	26	0.03	Spheres
$PLMA_{30}$-$PMMA_{70}$	90	98	19,500	1.13	39	0.07	Spheres and Short Worms
$PLMA_{30}$-$PMMA_{90}$	90	99	21,600	1.16	54	0.11	Spheres and Short Worms
$PLMA_{30}$-$PMMA_{110}$	90	98	22,100	1.17	55	0.11	Spheres and Short Worms
$PLMA_{30}$-$PMMA_{120}$	90	99	24,500	1.19	107	0.20	Spheres and Short Worms
$PLMA_{30}$-$PMMA_{140}$	90	99	26,700	1.20	145	0.24	Aggregated Spheres
$PLMA_{30}$-$PMMA_{150}$	90	99	28,200	1.23	362	0.59	Aggregated Spheres
$PLMA_{30}$-$PMMA_{200}$	90	98	32,600	1.28	892	0.45	Aggregated Spheres

Table S4. Summary of the GPC, DLS and TEM data obtained for a series of $PLMA_{41}$-$PMMA_x$ nano-objects prepared at 20% w/w solids in mineral oil at 90 °C using the two-pot protocol.

Target Composition	Synthesis Temperature (°C)	MMA Conversion (%)	THF GPC		DLS		TEM Morphology
			M_n (g mol^{-1})	M_w/M_n	D_h (nm)	PDI	
$PLMA_{41}$-$PMMA_{30}$	90	97	17,400	1.23	24	0.07	Spheres
$PLMA_{41}$-$PMMA_{40}$	90	97	18,900	1.15	27	0.03	Spheres
$PLMA_{41}$-$PMMA_{50}$	90	98	21,200	1.17	29	0.02	Spheres
$PLMA_{41}$-$PMMA_{70}$	90	97	23,400	1.17	32	0.04	Spheres
$PLMA_{41}$-$PMMA_{100}$	90	98	24,400	1.39	40	0.05	Spheres
$PLMA_{41}$-$PMMA_{120}$	90	98	26,700	1.20	46	0.07	Spheres
$PLMA_{41}$-$PMMA_{140}$	90	98	29,700	1.39	90	0.14	Spheres
$PLMA_{41}$-$PMMA_{160}$	90	98	31,500	1.38	120	0.17	Spheres
$PLMA_{41}$-$PMMA_{200}$	90	97	36,500	1.20	139	0.22	Spheres

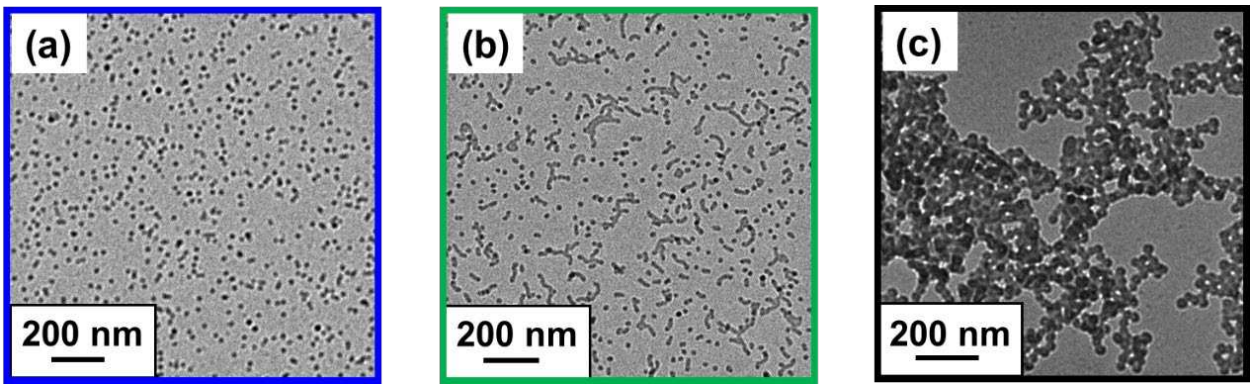

Figure S5. Representative TEM images of **(a)** the $PLMA_{19}$-$PMMA_{49}$ spheres **(b)** the $PLMA_{19}$-$PMMA_{69}$ mixture of short worms and spheres and **(c)** the $PLMA_{19}$-$PMMA_{198}$ large spherical aggregates prepared using the one-pot protocol at 20% w/w solids in mineral oil at 90 °C.

Table S5. Summary of the GPC, DLS and TEM data obtained for a series of $PLMA_{19}$-$PMMA_x$ nano-objects prepared using the one-pot protocol at 90 °C targeting either 30% w/w solids in mineral oil or 20% w/w solids in *n*-dodecane.

Target Composition	Solvent	MMA Conversion (%)	THF GPC		DLS		TEM Morphology
			M_n (g mol^{-1})	M_w/M_n	D_h (nm)	PDI	
$PLMA_{19}$	Mineral oil	-	6,400	1.12	-	-	-
$PLMA_{19}$-$PMMA_{30}$	Mineral oil	97	9,900	1.12	18	0.03	Spheres
$PLMA_{19}$-$PMMA_{60}$	Mineral oil	98	11,700	1.13	28	0.05	Spheres
$PLMA_{19}$-$PMMA_{100}$	Mineral oil	99	17,600	1.16	199	0.38	Short Worms and Spheres
$PLMA_{19}$-$PMMA_{200}$	Mineral oil	99	27,200	1.35	470	0.56	Aggregated Spheres
$PLMA_{19}$	*n*-dodecane	-	6,500	1.12	-	-	-
$PLMA_{19}$-$PMMA_{30}$	*n*-dodecane	96	11,200	1.15	19	0.03	Spheres
$PLMA_{19}$-$PMMA_{60}$	*n*-dodecane	97	14,200	1.15	24	0.03	Spheres
$PLMA_{19}$-$PMMA_{100}$	*n*-dodecane	98	17,400	1.16	29	0.03	Spheres
$PLMA_{19}$-$PMMA_{130}$	*n*-dodecane	98	18,400	1.19	44	0.08	Spheres and Short Worms
$PLMA_{19}$-$PMMA_{160}$	*n*-dodecane	98	21,500	1.21	84	0.14	Spheres and Short Worms
$PLMA_{19}$-$PMMA_{180}$	*n*-dodecane	98	21,800	1.23	133	0.24	Short Worms and Spheres
$PLMA_{19}$-$PMMA_{200}$	*n*-dodecane	98	26,300	1.23	1090	0.97	Aggregated Spheres

Table S6. Summary of the GPC, DLS and TEM data obtained for a series of $PSMA_{10}$-$PMMA_x$ nano-objects prepared using the two-pot protocol at 20% w/w solids in mineral oil at 90 °C.

Target Composition	Synthesis Temperature (°C)	MMA Conversion (%)	THF GPC		DLS		TEM Morphology
			M_n (g mol^{-1})	M_w/M_n	D_h (nm)	PDI	
$PSMA_{10}$	70	-	4,400	1.13	-	-	-
$PSMA_{10}$-$PMMA_{30}$	90	97	8,500	1.12	18	0.04	Spheres
$PSMA_{10}$-$PMMA_{50}$	90	98	10,600	1.14	26	0.04	Spheres
$PSMA_{10}$-$PMMA_{70}$	90	98	12,300	1.17	104	0.23	Short Worms
$PSMA_{10}$-$PMMA_{90}$	90	98	17,000	1.29	742	0.61	Spheres and Short Worms
$PSMA_{10}$-$PMMA_{110}$	90	98	16,900	1.24	678	0.49	Spheres and Short Worms
$PSMA_{10}$-$PMMA_{140}$	90	97	19,800	1.29	783	0.82	Aggregated Spheres
$PSMA_{10}$-$PMMA_{200}$	90	97	23,700	1.77	416	0.62	Aggregated Spheres

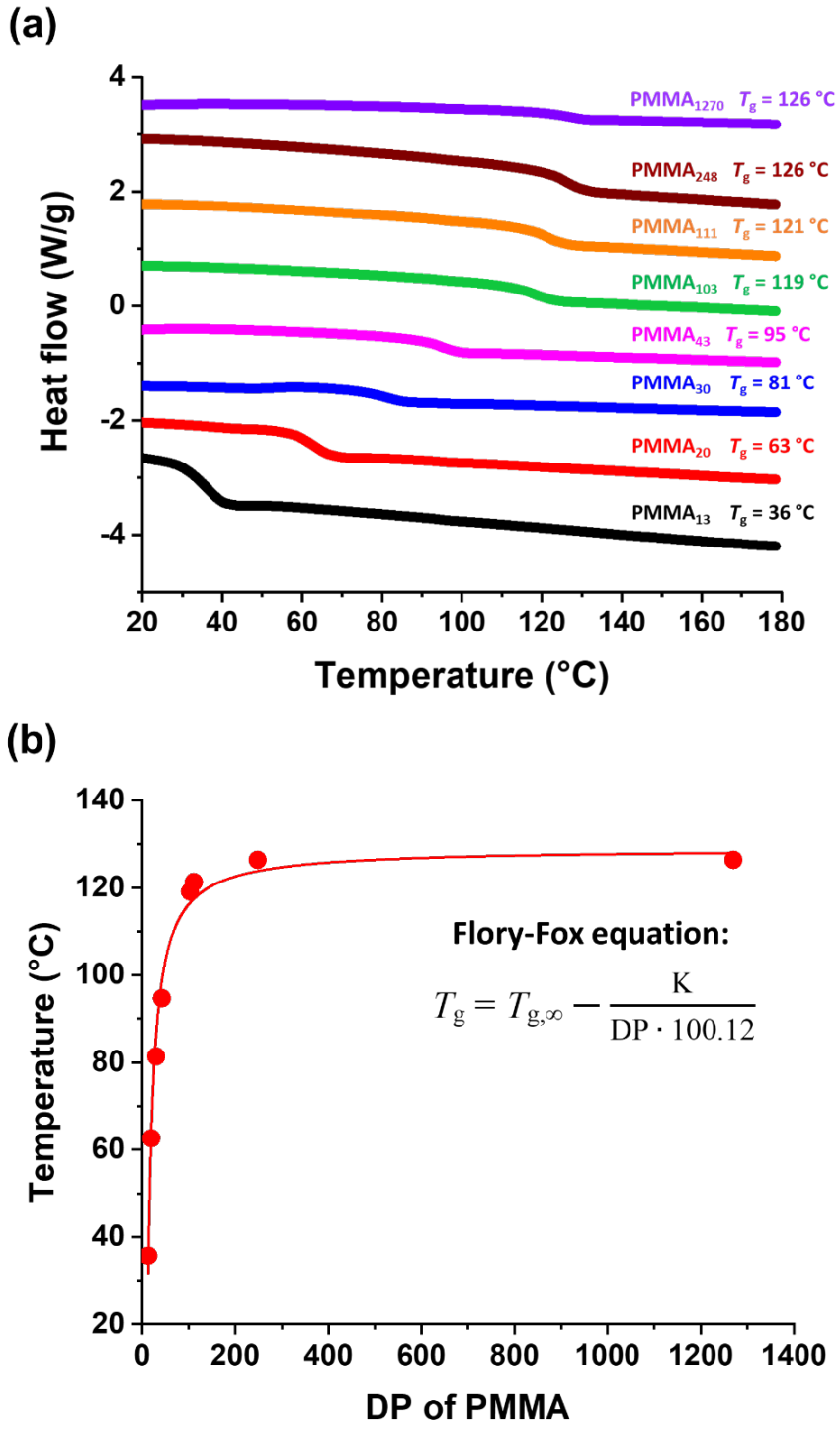

Figure S6. (a) DSC thermograms obtained for a series of near-monodisperse PMMA homopolymers with mean degrees of polymerization (DPs) ranging between 13 and 1270. **(b)** Plot of T_g against mean DP for the same series of PMMA homopolymers. Fitting the Fox-Flory equation to the data points (see red curve) gives $T_{g,\infty}$ = 129 ± 2 °C and K = 127 700 ± 5 700 g mol^{-1}.

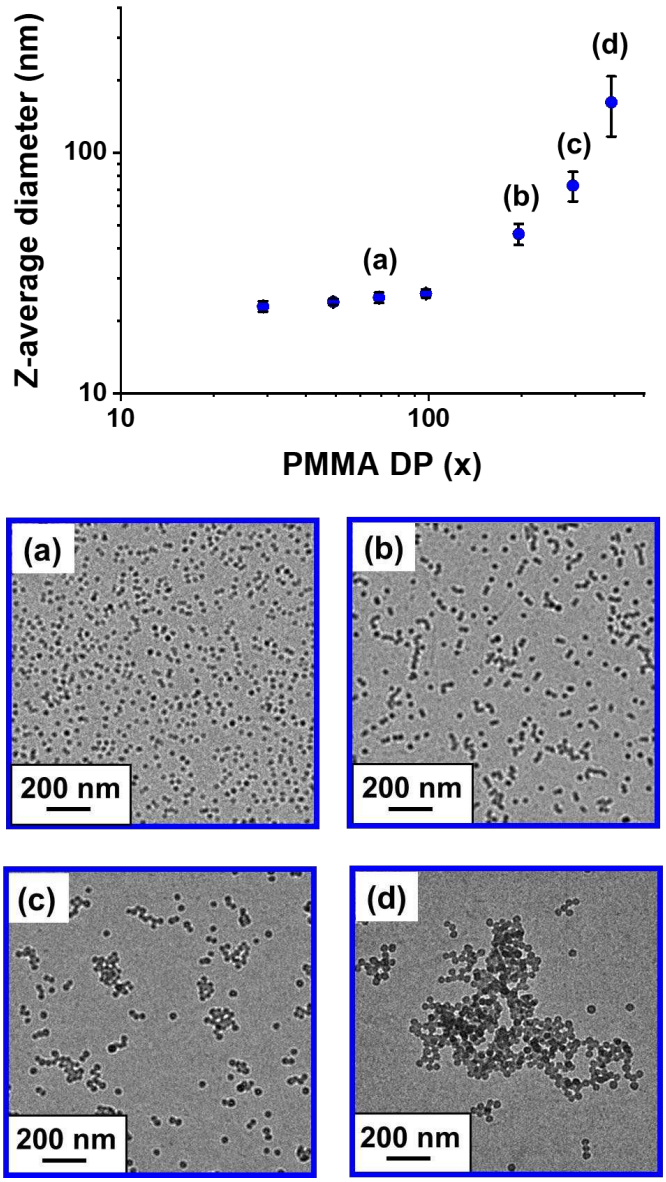

Figure S7. Double logarithmic plot for the relationship between z-average diameter and PMMA DP (x) for a series of $PSMA_{37}$-$PMMA_x$ (ranging x from 29 to 392) spheres prepared by RAFT dispersion polymerization of MMA at 90 °C in mineral oil targeting 20% w/w solids using the two-pot protocol. [N.B. Standard deviations are calculated from the DLS polydispersities and thus indicate the breadth of the particle size distributions, rather than the experimental error]. Representative TEM images obtained for **(a)** $PSMA_{37}$-$PMMA_{69}$ **(b)** $PSMA_{37}$-$PMMA_{196}$ **(c)** $PSMA_{37}$-$PMMA_{294}$ and **(c)** $PSMA_{37}$-$PMMA_{392}$ spherical nanoparticles. The apparent aggregation observed in (c) and (d) is consistent with the upturn in the DLS diameter observed above a PMMA Dp of 100 and indicates incipient flocculation for these larger spheres.

Table S7. Summary of the GPC, DLS and TEM data obtained for a series of $PSMA_{37}$-$PMMA_x$ nano-objects prepared using the two-pot protocol at 20% w/w solids in mineral oil at 90 °C.

Target Composition	Synthesis Temperature (°C)	MMA Conversion (%)	THF GPC		DLS		TEM Morphology
			M_n (g mol^{-1})	M_w/M_n	D_h (nm)	PDI	
$PSMA_{37}$	70	-	10,900	1.11	-	-	-
$PSMA_{37}$-$PMMA_{30}$	90	97	16,600	1.12	23	0.05	Spheres
$PSMA_{37}$-$PMMA_{50}$	90	97	18,800	1.13	24	0.03	Spheres
$PSMA_{37}$-$PMMA_{70}$	90	98	20,800	1.13	25	0.05	Spheres
$PSMA_{37}$-$PMMA_{100}$	90	98	21,600	1.14	26	0.04	Spheres
$PSMA_{37}$-$PMMA_{200}$	90	98	27,000	1.28	46	0.10	Spheres
$PSMA_{37}$-$PMMA_{300}$	90	98	37,300	1.38	73	0.14	Spheres
$PSMA_{37}$-$PMMA_{400}$	90	98	39,000	1.49	162	0.28	Spheres

Table S8. Summary of the GPC, DLS and TEM data obtained for a series of $PLMA_{22}$-$PMMA_x$ nano-objects prepared at 20% w/w solids in mineral oil at either 70 °C or 115 °C using the two-pot protocol.

Target Composition	Synthesis Temperature (°C)	MMA Conversion (%)	THF GPC		DLS		TEM Morphology
			M_n (g mol^{-1})	M_w/M_n	D_h (nm)	PDI	
$PLMA_{22}$-$PMMA_{30}$	70	98	9,600	1.11	19	0.10	Spheres
$PLMA_{22}$-$PMMA_{40}$	70	98	11,200	1.12	61	0.16	Spheres and Short Worms
$PLMA_{22}$-$PMMA_{60}$	70	96	12,300	1.14	250	0.58	Short Worms
$PLMA_{22}$-$PMMA_{70}$	70	98	14,400	1.16	470	0.60	Short Worms
$PLMA_{22}$-$PMMA_{120}$	70	96	19,000	1.30	1064	0.67	Aggregated Spheres
$PLMA_{22}$-$PMMA_{140}$	70	95	20,600	1.32	1932	0.99	Aggregated Spheres
$PLMA_{22}$-$PMMA_{200}$	70	95	24,000	1.37	1906	0.22	Aggregated Spheres
$PLMA_{22}$-$PMMA_{50}$	115	95	11,600	1.16	26	0.04	Spheres
$PLMA_{22}$-$PMMA_{70}$	115	97	14,000	1.16	29	0.02	Spheres
$PLMA_{22}$-$PMMA_{90}$	115	95	16,200	1.17	32	0.02	Spheres
$PLMA_{22}$-$PMMA_{120}$	115	95	19,700	1.17	36	0.03	Spheres
$PLMA_{22}$-$PMMA_{200}$	115	96	25,400	1.19	50	0.04	Spheres
$PLMA_{22}$-$PMMA_{300}$	115	97	33,100	1.24	123	0.19	Spheres
$PLMA_{22}$-$PMMA_{400}$	115	96	35,200	1.29	150	0.19	Spheres

Table S9. Summary of the structural parameters obtained from fitting SAXS patterns recorded for a series of PLMA$_{22}$-PMMA$_x$ nano-objects using either a spherical micelle or a worm-like micelle model.[6] D_{sphere} is the overall sphere diameter such that $D_{sphere} = 2R_s + 4R_g$, where R_s is the mean core radius and R_g is the radius of gyration of the stabilizer chains. T_{worm} is the overall worm thickness ($T_{worm} = 2R_{wc} + 4R_g$, where R_{wc} is the mean worm core radius) and L_{worm} is the mean worm contour length. N_{agg} is the mean aggregation number (*i.e.* the mean number of copolymer chains per nano-object).

Block copolymer	Copolymer Morphology	D_{sphere} (nm)	T_{worm} (nm)	L_{worm} (nm)	N_{agg}
PLMA$_{22}$-PMMA$_{29}$	Spheres	14.4 ± 2.6	-	-	193
PLMA$_{22}$-PMMA$_{69}$	Worms	-	14.2 ± 1.4	200	535
PLMA$_{22}$-PMMA$_{114}$	Spheres	29.2 ± 2.8	-	-	570
PLMA$_{22}$-PMMA$_{192}$	Spheres	39.2 ± 4.4	-	-	896

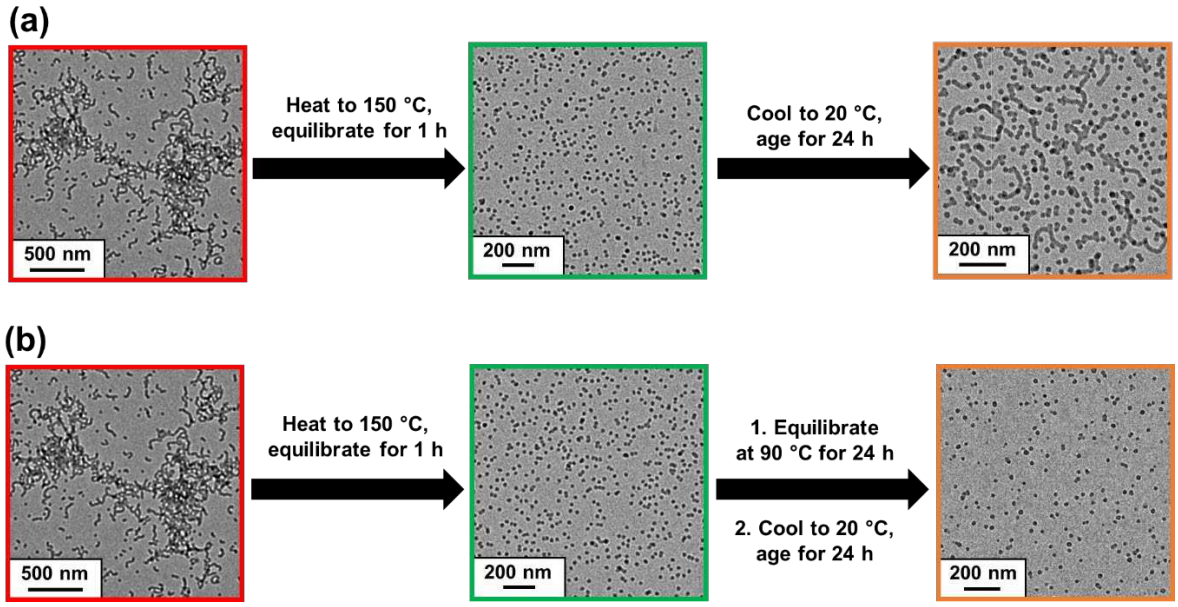

Figure S8. Representative TEM images recorded during the worm-to-sphere transition for the PLMA$_{22}$-PMMA$_{69}$ short worms prepared at 20% w/w solids in mineral oil. **(a)** This initial copolymer dispersion (red frame) was heated to 150 °C and equilibrated for 1 h at this temperature, prior to dilution with hot *n*-dodecane (green frame) and finally aged for 24 h at 20 °C (orange frame). **(b)** The same copolymer dispersion (red frame) was heated to 150 °C and equilibrated for 1 h at this temperature, prior to dilution with hot *n*-dodecane (green frame) followed by further equilibration at 90 °C for 24 h, cooling to 20 °C and ageing for 24 h (orange frame).

References

(1) György, C.; Hunter, S. J.; Girou, C.; Derry, M. J.; Armes, S. P. Synthesis of Poly(Stearyl Methacrylate)-Poly(2-Hydroxypropyl Methacrylate) Diblock Copolymer Nanoparticles via RAFT Dispersion Polymerization of 2-Hydroxypropyl Methacrylate in Mineral Oil. *Polym. Chem.* **2020**, *11*, 4579–4590.

(2) György, C.; Derry, M. J.; Cornel, E. J.; Armes, S. P. Synthesis of Highly Transparent Diblock Copolymer Vesicles via RAFT Dispersion Polymerization of 2,2,2-Trifluoroethyl Methacrylate in N-Alkanes. *Macromolecules* **2021**, *54*, 1159–1169.

(3) Fielding, L. A.; Lane, J. A.; Derry, M. J.; Mykhaylyk, O. O.; Armes, S. P. Thermo-Responsive Diblock Copolymer Worm Gels in Non-Polar Solvents. *J. Am. Chem. Soc.* **2014**, *136*, 5790–5798.

(4) Trent, J. S. Ruthenium Tetraoxide Staining of Polymers: New Preparative Methods for Electron Microscopy. *Macromolecules* **1984**, *17*, 2930–2931.

(5) Ilavsky, J.; Jemian, P. R. Irena: Tool Suite for Modeling and Analysis of Small-Angle Scattering. *J. Appl. Crystallogr.* **2009**, *42*, 347–353.

(6) Pedersen, J. S. Form Factors of Block Copolymer Micelles with Spherical, Ellipsoidal and Cylindrical Cores. *J. Appl. Crystallogr.* **2000**, *33*, 637–640.